skeletal muscle membranes (called primary dysferlinopathy).[2,5,6] Secondary dysferlin deficiency or altered localization due to mutation of the non-*DYSF* gene has also been reported in patients with dystrophinopathy,[7] sarcoglycanopathy,[7] caveolinopathy,[8–10] or calpainopathy[8,11–13] (often classified as secondary dysferlinopathy). Thus, the definitive diagnosis of dysferlinopathy requires identification of the *DYSF* mutation. Since 1998, our group has performed mutation analysis for *DYSF* in more than 160 families suspected of having dysferlinopathy using PCR–single-strand conformational polymorphism analysis or Sanger sequencing.[1,14,15] We previously identified >50 different mutations across the entire *DYSF* gene in approximately 60% of the patients.[1,14,15] We did not find *DYSF* mutations in the remaining approximately 40% of the patients, which suggests that these patients may have mutations in other myopathy-associated genes.

The aim of this study was to conduct targeted next-generation sequencing of myopathy-associated genes to reanalyze the patients with suspected dysferlinopathy who did not previously show *DYSF* mutations. This should enable us to reveal the genetic profile for myopathies with dysferlin deficiency.

METHODS Standard protocol approvals, registrations, and patient consents. This study was approved by the Ethics Committee of the Tohoku University School of Medicine, and all individuals gave their informed consent before their inclusion.

Patients. ***Cohort for targeted next-generation sequencing (cohort 1).*** PCR–single-strand conformational polymorphism analysis or Sanger sequencing of *DYSF* had previously been performed in 150 probands with suspected dysferlinopathy: 98 of them (65.3%) were diagnosed with *DYSF* mutations and 52 (34.7%) remained undiagnosed, with no pathogenic mutation in 43 and single heterozygous mutations in 9 (table e-1 at Neurology.org/ng). A total of 64 patients, including the above-mentioned prescreened but undiagnosed 52 patients and 12 newly enrolled patients, were analyzed using targeted next-generation sequencing. Of the 64 patients analyzed, a deficiency or reduction in sarcolemmal dysferlin was confirmed in 41 patients using immunohistochemical analysis of dysferlin in muscle samples (classified as "pathologically proven cases"), whereas dysferlin deficiencies were not confirmed in the remaining 23 patients, mainly because muscle biopsies or immunohistochemical analyses for dysferlin had not been performed (classified as "clinically suspected cases") (table 1). All of the 23 patients had teenage-to-adult–onset slowly progressive myopathy without predominant cardiac dysfunction or early-onset respiratory dysfunction with at least 1 of the dysferlinopathy-likely phenotypes: initial or strong involvement of the flexor muscles in distal lower limbs (15 of 23 patients) or a moderate-to-extreme increase (>1,000 IU/L) in serum creatine kinase (CK) levels (12 of 23 patients).

Cohort for analyzing the genetic profile in the pathologically proven cases (cohort 2). To analyze the genetic profile in

Table 1 Constitution and results for 2 cohorts

	Pathologically proven cases (cohort 2)		Clinically suspected cases		Total
Previously diagnosed cases		N = 49		N = 51	N = 100
	DYSF	47	*DYSF*	51	
	non-*DYSF*	2			
	CAPN3	1			
	CAV3	1			
Patients analyzed by targeted next-generation sequencing (cohort 1)		N = 41		N = 23	N = 64
	DYSF	16[a]	*DYSF*	7	23[a] (table 3)
	non-*DYSF*	12[a]	non-*DYSF*	4	16[a] (table 4)
	CAPN3	8	*CAPN3*	2	
	DYSF/MYOT/CAV3	1[a]	*GNE*	1	
	CAV3	1	*MYH2*	1	
	ANO5	1			
	GNE	1			
	Undiagnosed	14	Undiagnosed	12	26
Total		N = 90		N = 74	N = 164

[a] Includes 1 patient (Dys149-1) with putative pathogenic mutations detected in *DYSF*, *MYOT*, and *CAV3*, who was counted in both *DYSF* and non-*DYSF* groups.

the pathologically proven cases, the 47 patients with previously identified *DYSF* mutations[1,14,15] and the 2 patients with *CAPN3* and *CAV3*[10] mutations were combined with the aforementioned 41 undiagnosed but pathologically proven cases, amounting to a total of 90 patients in this cohort (table 1).

Immunohistochemical analysis for dysferlin. Immunohistochemical analysis for dysferlin in muscle samples was performed in the institution or hospital that the patient visited. Although the detailed methods may not have been identical in all cases, most cases were investigated by the avidin–biotin–peroxidase complex immunostaining method using the mouse monoclonal antibody to dysferlin (NCL-Hamlet; Leica Biosystems, Wetzlar, Germany) as the primary antibody.

Targeted next-generation sequencing. We selected 42 genes that have been reported to cause adult-onset myopathy or muscular dystrophy (table 2). The targeted regions were designed using the SureDesign system (Agilent Technologies, Santa Clara, CA) to include all coding exons with 3′ and 5′ intronic 25-bp flanking bases (the regional source for coding exons was extracted from RefSeq, CCDS, Ensemble, Gencode, or Vega databases) and 3′ and 5′ untranslated regions. The targeted region for *DYSF* was designed to include 58 exons (i.e., exon 1–55, the alternative first exon, and exons 5a and 40a) to cover all alternative spliced variants. Of the total targeted region of 498.98 kb, 488.98 kb (98.08% coverage) was expected to be covered by 17,143 amplicons. Genomic DNA from the targeted region was captured using the HaloPlex target-enrichment system (Agilent Technologies). Targeted libraries were sequenced using the MiSeq platform, according to the manufacturer's instructions (Illumina, San Diego, CA). Paired 151-bp reads were aligned to the reference human genome (UCSChg19) using the Burrows–Wheeler Alignment tool.[16] Single-nucleotide variants and indels were identified using the Genome Analysis Toolkit v1.5.[17] Single-nucleotide variants and indels were annotated against the RefSeq and Single Nucleotide Polymorphism databases (dbSNP137) in the ANNOVAR program.[18] We used the PolyPhen-2 polymorphism phenotyping software tool and SIFT[19,20] to predict the functional effects of mutations and eXome-Hidden Markov Model (XHMM, http://atgu.mgh.harvard.edu/xhmm/) to call copy-number variations. We extracted variations that were listed as myopathy-causing mutations in the Human Gene Mutation Database (HGMD; provided by BIOBASE, Waltham, MA). For further analysis, we filtered variations satisfying all of the following conditions: variations located in exon or splice sites that were not detected in the control DNA included in the HaloPlex target enrichment system, variations that were covered by a minimum of 20 reads with a genotype quality score of at least 80, and variations with an altered allele frequency that ranged from 0.3 to 0.7 in the heterozygous state or that was greater than 0.7 in the homozygous state. Among these, nonsynonymous variants that either were absent or had a frequency of <1% in both the 1000 Genomes Database and the Human Genetic Variation Database (http://www.genome.med.kyoto-u.ac.jp/SnpDB/) were left as rare variants.

Sanger sequencing. We performed Sanger sequencing to confirm that the mutations identified by exome sequencing segregated with the disease. PCR products were purified using a MultiScreen-PCR plate (Millipore, Billerica, MA) followed by sequencing with a 3500xL Genetic Analyzer (Thermo Fisher Scientific, Waltham, MA).

Multiplex ligation-dependent probe amplification. To investigate copy-number variation in *DYSF*, we performed multiplex ligation-dependent probe amplification (MLPA) with SALSA MLPA probemix P268-A1 DYSF (MRC Holland, Amsterdam, the Netherlands) according to the manufacturer's instructions. This MLPA design contains probes to amplify 40 of the 58 exons. Genomic DNA (50–250 ng) was hybridized using the probemix. After ligation and amplification, the PCR products were separated by size using a 3130xL Genetic Analyzer (Thermo Fisher Scientific). Relative peak areas were calculated with GeneMapper software (Thermo Fisher Scientific).

Subcloning. To investigate the allelic condition of multiple heterozygous mutations in a particular gene, we performed subcloning of PCR products. Long-range PCR was performed under optimized long-PCR conditions using LA Taq polymerase (Takara, Shiga, Japan). The PCR products were subcloned into the vector pCR2.1 TOPO (Invitrogen, Waltham, MA). Several clones were randomly picked from each bacterial culture, and DNA was extracted for Sanger sequencing.

RESULTS

Targeted next-generation sequencing. An average of 96.8% (92.6%–98.2%) and 93.7% (84.6%–97.6%) of the overall targeted regions had at least 10- and 30-fold coverage, respectively (table e-2). The average read depth calculated for each gene ranged from 207 (*GFPT1*) to 429 (*CAV3*). An average of 89.7% (*FKRP*) to 99.9% (*CAPN3*) of the targeted regions had at least 10-fold coverage, and 83.1% (*FKRP*) to 99.4% (*TRIM32*) of the targeted regions had at least 30-fold coverage. These regions corresponded to those estimated to have been uncaptured by any amplicon. The sequencing data covered 99.4% and 98.1% of the targeted *DYSF* region with at least 10- and 30-fold coverage, respectively, with an average read depth of 388.

With reference to the HGMD, 0–3 myopathy-causing mutations were extracted per individual. After filtering with the quality-related and frequency thresholds described earlier, 0–17 rare nonsynonymous variants remained per individual. After considering the predicted functional effect, pattern of inheritance, and clinical information, putative pathogenic variants were detected in 38 of 64 patients (26 of 52 prescreened undiagnosed patients and all 12 newly enrolled patients).

Twenty-three of the 38 mutation-positive patients (12 of 52 prescreened undiagnosed patients and 11 of 12 newly enrolled patients) had *DYSF* mutations; these included 6 novel mutations (tables 1 and 3). Novel homozygous deletion of exons 37 and 38 (Dys194-1) and heterozygous deletion of exons 37 to 41 (Dys119-1-2) were predicted by XHMM software and confirmed by MLPA and Sanger sequencing, which revealed deletions of 5,862 and 51,161 bps, respectively.

The remaining 16 patients (15 of 52 prescreened undiagnosed patients and 1 of 12 newly enrolled patients), including a single patient (Dys149-1) in whom the *DYSF* mutation was simultaneously detected, were revealed to harbor known or rare

Table 2 The 42 myopathy-associated genes targeted in this study

Gene symbol	Position	Representative phenotype	OMIM no.	RefSeq no.	No. of coding exons	Transcript length, bp	Protein (aa)
ANO5	11p14.3	LGMD2L	611307	NM_213599	22	6,651	913
BAG3	10q25.2-q26.2	Myopathy, myofibrillar, 6	612954	NM_004281	4	2,571	575
CAPN3	15q15.1-q15.3	LGMD2A	253600	NM_000070	24	3,228	821
CAV3	3q25	LGMD1C	607801	NM_033337	2	1,431	151
COL6A1	21q22.3	Bethlem myopathy	158810	NM_001848	35	4,238	1,028
COL6A2	21q22.3	Bethlem myopathy	158810	NM_001849	28	3,461	1,019
COL6A3	2q37	Bethlem myopathy	158810	NM_004369	44	10,749	3,177
CRYAB	11q22.3-q23.1	Myopathy, myofibrillar, 2	608810	NM_001289807	3	1,017	175
DAG1	3p21.31	LGMD2P	613818	NM_001177634	6	5,829	895
DES	2q35	LGMD2R	615325	NM_001927	9	2,248	470
DNAJB6	7q36.3	LGMD1E	603511	NM_058246	10	2,527	326
DNM2	19q13.2	Myopathy, centronuclear	160150	NM_004945	20	3,588	866
DYSF	2p13.3-p13.1	LGMD2B	253601	NM_003494	55	6,796	2,080
EMD	Xq28	Emery-Dreifuss muscular dystrophy 1, X-linked	310300	NM_000117	6	1,379	254
FHL1	Xq27.2	Emery-Dreifuss muscular dystrophy 6, X-linked	300696	NM_001159704	6	2,888	280
FKRP	19q13.3	LGMD2I	607155	NM_024301	4	3,332	495
FKTN	9q31	LGMD2M	611588	NM_006731	10	7,364	461
FLNC	7q32	Myopathy, myofibrillar, 5	609524	NM_001458	48	9,188	2,725
GFPT1	2p13	Myasthenia, congenital, with tubular aggregates 1	610542	NM_001244710	20	8,703	699
GNE	9p13.3	Inclusion body myopathy, autosomal recessive	600737	NM_001128227	12	5,298	753
KLHL9	9p22	Early-onset distal myopathy	NA	NM_018847	1	5,710	617
LDB3	10q22.2-q23.3	Myopathy, myofibrillar, 4	609452	NM_001171610	14	5,436	732
LMNA	1q21.2	LGMD1B	159001	NM_170707	12	3,190	664
MATR3	5q31.2	Amyotrophic lateral sclerosis 21	606070	NM_001194954	18	5,604	847
MYH2	17p13.1	Inclusion body myopathy 3	605637	NM_017534	40	6,339	1,941
MYH7	14q12	Laing distal myopathy	160500	NM_000257	40	6,087	1,935
NEB	2q22	Nemaline myopathy 2, autosomal recessive	256030	NM_004543	150	20,637	6,669
PLEC1	8q24	LGMD2Q	613723	NM_000445	33	14,787	4,574
POMGNT1	1p34-p33	LGMD2O	613157	NM_001243766	23	2,934	748
POMT1	9q34.1	LGMD2K	609308	NM_001136113	20	3,320	725
POMT2	14q24.3	LGMD2N	613158	NM_013382	21	4,876	750
SGCA	17q12-q21.33	LGMD2D	608099	NM_000023	10	1,432	387
SGCB	4q12	LGMD2E	604286	NM_000232	6	4,431	318
SGCD	5q33	LGMD2F	601287	NM_000337	9	1,606	290
SGCG	13q12	LGMD2C	253700	NM_000231	8	1,624	291
TCAP	17q12	LGMD2G	601954	NM_003673	2	2,123	167
TPM2	9p13.2-p13.1	Nemaline myopathy 4, autosomal dominant	609285	NM_003289	9	1,189	284
TPM3	1q22-q23	Nemaline myopathy 1, autosomal dominant or recessive	609284	NM_001278188	8	3,131	248
TRIM32	9q31-q34.1	LGMD2H	254110	NM_012210	2	3,717	653
TTID	5q31	LGMD 1A	159000	NM_006790	10	2,337	498
TTN	2q31	LGMD2J	608807	NM_001267550	363	109,224	35,991
VCP	9p13-p12	Inclusion body myopathy with early-onset Paget disease and frontotemporal dementia 1	167320	NM_007126	17	4,370	806

Abbreviations: LGMD = limb-girdle muscular dystrophy; NA = not available.

Table 3 Summary of known or putative pathogenic *DYSF* mutations detected in this study

ID	Zygosity	Mutation type	Nucleotide change	Protein change	Listed in HGMD	dbSNP137	MAF in 1000 Genomes	MAF in HGVD	SIFT[a]	PolyPhen-2[b]
Pathologically proven cases										
Dys92-1	Het	Missense	c.356T>C	p.L119P	No		NA	NA	D	D
	Het	Missense	c.2997G>T	p.W999C	Yes	rs28937581	NA	NA	D	D
Dys129-1	Het	Nonsense	c.3444_3445delinsAA	p.Y1148X	Yes		NA	NA		
	Het	Nonsense	c.5903G>A	p.W1968X	Yes		NA	NA		
Dys149-1	Hom	Missense	c.1667T>C	p.L556P	Yes	rs200916654	0.0005	NA	D	P
Dys154-1	Hom	Nonsense	c.6135G>A	p.W2045X	Yes		NA	NA		
Dys166-1	Het	Frameshift	c.4200delC	p.P1400Pfs48X	Yes		NA	NA		
	Het	Missense	c.3118C>T	p.R1040W	Yes		NA	NA	D	D
Dys168-1	Het	Nonsense	c.2494C>T	p.Q832X	Yes	rs199543257	0.0005	NA		
	Het	Missense	c.2974T>C	p.W992R	Yes		NA	NA	D	D
Dys192-1	Hom	Missense	c.5078G>A	p.R1693Q	Yes		NA	NA	D	D
Dys194-1	Hom	Gross deletion	exon37-38del[c]		No		NA	NA		
Dys119-1-2	Het	Gross deletion	exon37-41del[d]		No		NA	NA		
	Het	Nonsense	c.3244G>T	p.E1082X	No		NA	NA		
Dys211-1	Het	Missense	c.2997G>T	p.W999C	Yes	rs28937581	NA	NA	D	D
	Het	Missense	c.5077C>T	p.R1693W	Yes		NA	NA	D	D
Dys213-1	Hom	Splicing	c.2644-2A>G		Yes		NA	0.001166		
Dys215-1	Het	Nonsense	c.1566C>G	p.Y522X	Yes		NA	NA		
	Het	Nonsense	c.2494C>T	p.Q832X	Yes	rs199543257	0.0005	NA		
Dys216-1	Hom	Missense	c.2974T>C	p.W992R	Yes		NA	NA	D	D
Dys218-1	Het	Splicing	c.663+1G>C		Yes		NA	NA		
	Het	Missense	c.2997G>T	p.W999C	Yes	rs28937581	NA	NA	D	D
Dys219-1	Het	Missense	c.2974T>C	p.W992R	Yes		NA	NA	D	D
	Het	Frameshift	c.3373delG	p.E1125Kfs9X	Yes		NA	NA		
Dys220-1	Hom	Nonsense	c.1566C>G	p.Y522X	Yes		NA	NA		
Clinically suspected cases										
Dys71-1	Het	Missense	c.356T>C	p.L119P	No		NA	NA	D	D
	Het	Missense	c.2997G>T	p.W999C	Yes	rs28937581	NA	NA	D	D
Dys116-1	Het	Missense	c.565C>G	p.L189V	Yes	rs13407355	0.02	0.020276	T	B
	Het	Missense	c.5873C>T	p.S1958F	No		NA	0.001166	D	D
	Het	Nonsense	c.6135G>A	p.W2045X	Yes		NA	NA		

Continued

Table 3 Continued

ID	Zygosity	Mutation type	Nucleotide change	Protein change	Listed in HGMD	dbSNP137	MAF in 1000 Genomes	MAF in HGVD	SIFT[a]	PolyPhen-2[b]
Dys132-1	Hom	Missense	c.1667T>C	p.L556P	Yes	rs200916654	0.0005	NA	D	P
Dys155-1	Hom	Nonsense	c.5713C>T	p.R1905X	Yes	rs121908959	NA	NA		
Dys207-1	Hom	Splicing	c.2643+1G>A		Yes	rs140108514	NA	NA		
Dys208-1	Hom	Missense	c.1663C>T	p.R555W	Yes		NA	NA	D	D
Dys210-1	Het	Missense	c.6196G>A	p.A2066T	Yes		NA	NA	T	B
	Het	Frameshift	c.5900delG	p.G1967Afs6X	No		NA	NA		

Abbreviations: HGMD = Human Gene Mutation Database; HGVD = Human Genetic Variation Database; Het = heterozygous; Hom = homozygous; MAF = minor allele frequency; NA = not available.
[a] SIFT scores are described as D = deleterious (SIFT ≤ 0.05); T = tolerated (SIFT >0.05).
[b] PolyPhen-2 (pp2_hvar) scores are described as D = probably damaging (≥0.909); P = possibly damaging (0.447 ≤ pp2_hdiv ≤ 0.909); B = benign (pp2_hdiv ≤ 0.446).
[c] Mutations are described according to NM_003494.3: c.3903+3532_c.4167+572del5862.
[d] Mutations are described according to NM_003494.3: c.3903+1161_c.4510-1036del51161.

mutations in non-*DYSF* genes (tables 1 and 4). Of these, novel or known mutations in *CAPN3* were detected in 10 patients, accounting for the majority of non-*DYSF* genes. The heterozygous p.V805A mutation in *MYH2*, which is a known mutation leading to inclusion body myositis,[21] was detected in Dys86-1. The pathogenicity of this mutation remained uncertain because of the lack of relevant information in muscle pathology.

Subsequently, MLPA was performed for the remaining 27 patients (table e-1), including all 14 patients who were undiagnosed after targeted sequencing but were pathologically proven, through targeted next-generation sequencing. We detected no additional duplications or deletions in *DYSF* (table e-1).

Genetic profile for pathologically proven cases. Figure 1 shows the genetic profile of the 90 pathologically proven cases (patients who showed sarcolemmal dysferlin deficiency in immunohistochemical analyses). Intriguingly, the 63 patients (47 previously diagnosed patients and 16 newly diagnosed patients) with *DYSF* mutations accounted for only 70% of cases, *CAPN* mutations accounted for 10% of cases (9/90), and *CAV3* mutations accounted for 2% of cases (2/90). The other genetic profile included mutations in *ANO5*, *GNE*, and *MYOT* (together with *CAV3* and *DYSF*), each of which was detected in a single individual. Clinical information for the remaining 14 patients who showed secondary dysferlin deficiency due to putative pathogenic mutations in non-*DSYF* genes is summarized in table 5.

DISCUSSION We performed targeted next-generation sequencing of 42 myopathy-associated genes in 64 patients with clinically or pathologically suspected dysferlinopathy. We found possible pathogenic mutations in *DYSF* or other genes in 38 patients (59.4%). The use of this targeted resequencing technique improved positive genetic detection from 65.3% (98/150 patients) to 82.7% (124/150 patients) overall, owing to (1) the detection of previously unrevealed *DYSF* mutations, including gross deletions, and (2) the comprehensive sequencing of non-*DYSF* genes and the detection of novel or known mutations in these genes.

Although secondary dysferlin deficiency can be caused by *CAPN3* mutations,[11–13] the exact frequency of *CAPN3* mutations in patients with dysferlin deficiency has not been reported previously. Human *CAPN3* is located on chromosome 15q15.1-15.3, comprises 24 exons, and codes a Ca^{2+}-dependent cysteine protease called calpain 3 (p94). Across the entire *CAPN3* gene, nearly 300 mutations have been reported to be pathogenic and the cause of LGMD2A (OMIM #253600),[22] which is estimated to be the most frequent type of LGMD in the Japanese

Table 4 Summary of known or putative pathogenic non-*DYSF* mutations detected in this study

ID	Gene	Zygosity	Mutation type	Nucleotide change	Protein change	Listed in HGMD	dbSNP137	MAF in 1000 genomes	MAF in HGVD	SIFT[a]	PolyPhen-2[b]
Pathologically proven cases											
Dys76-1	*CAPN3*	Het	Missense	c.2105C>T	p.A702V	Yes		NA	NA	D	D
			Missense	c.2120A>G	p.D707G	Yes	rs200379491	0.0005	0.005	D	D
Dys79-1	*CAPN3*	C/H	Missense	c.992T>A	p.V331D	No		NA	NA	D	D
			Splicing	c.1194-9A>G		Yes		NA	0.001166		
Dys81-1	CAPN3	Hom	Missense	c.1524+1G>T		Yes		NA	NA		
Dys88-1	*CAPN3*	C/H	Missense	c.1435A>G	p.S479G	Yes	rs201736037	NA	NA	D	P
			Nonsense	c.1786A>T	p.K596X	No		NA	NA		
Dys91-1	*GNE*	Hom	Missense	c.1714G>C	p.V572L	Yes	rs121908632	0.0005	0.004283	D	D
Dys112-1	*CAPN3*	Hom	Missense	c.1381C>T	p.R461C	Yes		NA	0.002232	D	D
Dys149-1	*MYOT*	Het	Missense	c.1214G>A	p.R405K	Yes		NA	NA	T	B
	CAV3	Het	Missense	c.40G>A	p.V14I	No	rs121909281	0.0014	0.001255	T	B
Dys185-1	*PLEC*	Hom	Splicing	c.4126-4A>G		Yes	rs7002152	0.25	0.188366		
Dys189-1	*CAPN3*	C/H	Missense	c.2120A>G	p.D707G	Yes	rs200379491	0.0005	0.005	D	D
			Frameshift	c.2287_2288del	p.Y763X	No		NA	NA		
Dys195-1	*CAPN3*	Hom	Frameshift	c.7delA	p.T3Pfs54X	No		NA	NA		
Dys201-1	*ANO5*	Hom	Splicing	c.180+2T>C		No		NA	NA		
Dys203-1	*CAV3*	Het	Missense	c.122T>C	p.F41S	No		NA	NA	D	D
Dys214-1	*CAPN3*	C/H	Splicing	c.1194-9A>G		Yes		NA	0.001166		
			Missense	c.1742C>G	p.S581C	Yes		NA	0.013158	D	D
Clinically suspected cases											
Dys45-1	*GNE*	Het	Missense	c.1714G>C	p.V572L	Yes	rs121908632	0.0005	0.004283	D	D
			Del/ins	c.907_908delinsGT	p.C303V	Yes	rs121908633	NA	NA	D	P
Dys53-1	*CAPN3*	Het	Missense	c.1202A>G	p.Y401C	Yes		NA	0.001166	D	D
			Missense	c.1892A>G	p.D631G	No		NA	NA	D	B
Dys86-1	*MYH2*	Het	Missense	c.2414T>C	p.V805A	Yes	rs200662973	0.0018	0.009337	T	B
Dys188-1	*CAPN3*	Het	Missense	c.1465C>T	p.R489W	Yes		NA	NA	D	D
			Missense	c.1892A>G	p.D631G	No		NA	NA	D	B

Abbreviations: C/H = compound heterozygous; HGMD = Human Gene Mutation Database; HGVD = Human Genetic Variation Database; Het = heterozygous; Hom = homozygous; MAF = minor allele frequency; NA = not available.

Mutations are described according to the following RefSeq numbers. *ANO5*: NM_213599, *BAG3*: NM_004281.3, *CAPN3*: NM_000070, *CAV3*: NM_033337, *FKRP*: NM_024301.4, *GNE*: NM_005476, *MYOT*: NM_006790, *MYH2*: NM_017534, *PLEC*: NM_000445.3.

[a] SIFT scores are described as D = deleterious (SIFT ≤ 0.05); T = tolerated (SIFT > 0.05).

[b] PolyPhen-2 (pp2_hvar) scores are described as D = probably damaging (≥0.909); P = possibly damaging (0.447 ≤ pp2_hdiv ≤ 0.909); B = benign (pp2_hdiv ≤ 0.446).

Figure 1 Genetic profile of 90 patients with dysferlin deficiency

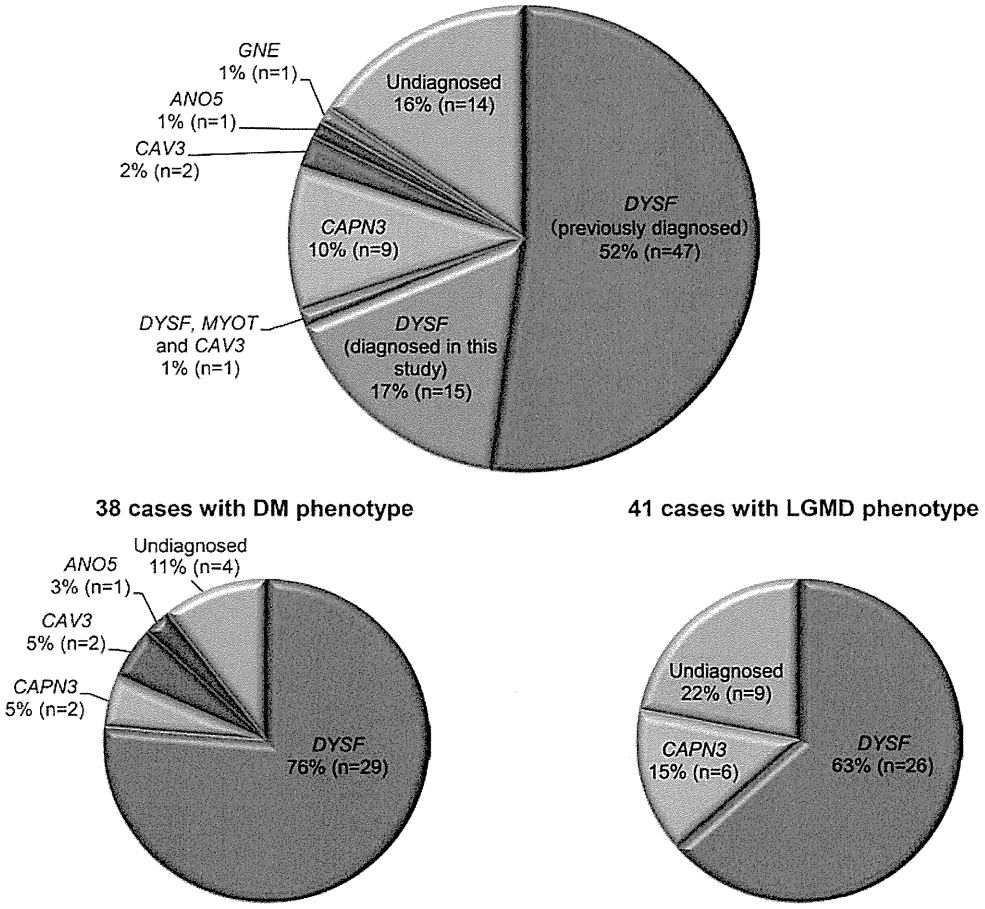

DYSF mutations were identified in a total of 63 patients (70%). Nine patients (10%) were diagnosed with *CAPN3* mutations. Of the 90 patients, 38 and 41 manifested as distal myopathy (DM) and limb-girdle muscular dystrophy (LGMD), respectively, and the remaining 11 were unclassifiable. The genetic profiles for each manifestation are also shown. The proportion of *DYSF* mutations was more frequent for the DM phenotype (76%) than for the LGMD phenotype (63%), whereas *CAPN3* mutations were more frequent in the LGMD phenotype (15%) than in the DM phenotype (5%).

population.[8] In this study, although mutations in *CAPN3* were essentially distributed sporadically, thus not suggesting a specific genotype to associate with dysferlin deficiency, our result of 10% frequency in *CAPN3* mutations with dysferlin deficiency emphasizes the necessity for genetic analysis of both genes.

Clinically, 2 of the 9 patients with *CAPN3* mutations manifested atypically with a distal myopathy (DM) phenotype rather than LGMD (figure 1, table 5). One of the patients with DM (Dys189-1) had weakness of the tibialis anterior muscle as an initial symptom and showed gastrocnemius muscle atrophy, closely resembling MMD1 (table 5).

Immunohistochemistry for calpain 3 revealed reduced expression in this patient. The other patient (Dys88-1) also had distal weakness with wasting, particularly in the tibialis anterior muscle. Although immunohistochemistry for calpain 3 was rarely investigated in our cases of dysferlinopathy, a secondary reduction in calpain 3 with *DYSF* mutations has also been reported.[23] These findings indicate that it is difficult to distinguish calpainopathy from dysferlinopathy, even when considering clinical information together with immunohistochemical analysis of both proteins. Genetic analysis of both genes would be valuable for genetic counseling, clinical management,[24] and possible specific genetic therapies in the future.

Non-*DYSF* and non-*CAPN3* genes were responsible for 5% of patients with dysferlin deficiencies (figure 1, table 5). A novel *CAV3* mutation was identified in Dys203-1, and immunohistochemical analyses in this patient showed reduced expression of both dysferlin and caveolin, confirming the diagnosis. Together with the known homozygous p.L556P mutation in *DYSF*, a known heterozygous p.R405K mutation in *MYOT* and a rare mutation of p.V14I in *CAV3* were detected in 1 patient (Dys149-1). This

Table 5 **Clinical characteristics for the 14 patients who showed secondary dysferlin deficiency**

ID	Gene	Mutation	Sex, population, family history	Initial manifestation	Phenotype	Distribution of affected muscles	Serum CK, IU/L	Muscle pathology	Immunohistochemical detection of dysferlin
Dys201-1	*ANO5*	Hom, c.180+2T>C	Male, Japanese, sporadic	54 y, walking disability	DM	GC, BF, AM	4,489	Inflammation and degeneration	Reduced expression (figure e-1)
Dys70-1	*CAV3*	Het, p.R27Q	Female, Japanese, sporadic	12 y, hyperCK	DM	Small muscles of hands and feet	2,092	Mild myopathic change and type 1 fiber predominance	Reduced expression (not shown)
Dys203-1	*CAV3*	Het, p.F41S	Male, Japanese, sporadic	43 y, hyperCK	DM	GC, RF, Ham	2,295	Degeneration with RVs and neuropathic change	Reduced expression (figure e-1)
Dys189-1	*CAPN3*	C/H, p.D707G, p.763_763del	Male, Japanese, sister	19 y, walking disability	DM	TA, IP (weakness); GC, BF (atrophy)	3,695	Mild myopathic change	Reduced expression (figure e-1)
Dys195-1	*CAPN3*	Hom, p.T3fs	Female, Egyptian, brother	NA	NA	NA	NA	Inflammation	Absent (not shown)
Dys214-1	*CAPN3*	C/H, c.1194-9A>G, p.S581C	Female, Japanese, sporadic	Childhood, walking disability	LGMD	Proximal and lower limb dominant	3,324	NA	Reduced expression (not shown)
Dys76-1	*CAPN3*	Possible C/H, p.A702V, p.D707G	Female, Japanese, sporadic	28 y, walking disability	LGMD	Diffuse	1,000-3,000	Degeneration	Reduced expression (not shown)
Dys79-1	*CAPN3*	C/H, c.1194-9A>G, p.V331D	Male, Japanese, sporadic	18 y, walking disability	LGMD	Proximal dominant with scapular wing	1,992	Degeneration with lobulated fibers	Reduced expression (not shown)
Dys81-1	*CAPN3*	Hom, c.1524+1G>T	Female, Japanese, brother	18 y, walking disability	LGMD	Proximal dominant	115	Degeneration	Reduced and mosaic expression (not shown)
Dys88-1	*CAPN3*	Possible C/H, p.S479G, p.K596X	Female, Australian, cousin	NA	DM	TA	NA	NA	Reduced expression (not shown)
Dys112-1	*CAPN3*	Hom, p.R461C	Male, Japanese, sporadic	43 y, grip weakness	Unclassifiable	BB	1,500	Dystrophic change	Reduced expression (not shown)
Dys209-1	*CAPN3*	Hom, c.1194-9A>G	Female, Japanese, sporadic	Childhood, walking disability	LGMD	Proximal dominant	261	Mild degeneration	Reduced expression (not shown)
Dys91-1	*GNE*	Hom, p.V572L	Male, Japanese, NA	NA	NA	NA	NA	RVs	Partial reduction (not shown)
Dys149-1	*MYOT*, *CAV3*	Het, p.R405K Het, p.V14I	Male, Japanese, sporadic	18 y, hyperCK	NA	No weakness or atrophy	>20,000	NA	Absent (figure e-1)

Abbreviations: AM = adductor magnus; BB = biceps brachii; BF = biceps femoris; C/H = compound heterozygous; CK = creatine kinase; DM = distal myopathy; GC = gastrocnemius; GM = gluteus maxim; Ham = hamstrings; Het = heterozygous; Hom = homozygous; IP = iliopsoas; LGMD = limb-girdle muscular dystrophy; NA = not available; RF = rectus femoris; RV = rimmed vacuole; TA = tibialis anterior.

patient was a sporadic case with isolated hyperCKemia. Thus, it is unknown whether the muscle pathology showing absent dysferlin was caused by the *DYSF* mutation or by the associated effects of multiple mutations. A novel homozygous *ANO5* splicing mutation was identified in Dys201-1. *ANO5* encodes the transmembrane protein anoctamin 5 and is the causative gene for MMD3 (OMIM #613319) and LGMD2L (OMIM #611307). Asymmetrical muscle atrophy was predominantly observed in the gastrocnemius, biceps femoris, and adductor magnus in this patient and is a possible distribution in both MMD1 and MMD3.[25] Expression of dysferlin in this patient was diffusely decreased, mimicking MMD1 (figure e-1). A homozygous *GNE* mutation was detected in Dys91-1, compatible with DM with rimmed vacuoles, and this patient had a partial reduction in dysferlin (figure e-1). Secondary dysferlin deficiency from mutations in *ANO5* or *GNE* has not been reported previously. Hence, further investigations are required to clarify the possible association between these mutations and dysferlin deficiency.

Even after the targeted next-generation sequencing, 26 of 64 patients (40.6%) remained undiagnosed. This means that undiagnosed patients accounted for 15.6% of pathologically proven cases (14/90 patients) and 16.2% of clinically suspected cases (12/74 patients), showing nonsignificant difference between the 2 groups (table 1). There are several possible explanations: (1) mutations in subtle unsequenced targeted regions were not detected in this study; (2) intronic *DYSF* mutations that might result in abnormal splicing were not detected because these regions, along with messenger RNA, were not investigated; (3) pathogenic mutations were excluded because of biased filtering or overfiltering; or, most probably; (4) other genes not targeted in this study may be responsible. More than 50 molecules have been reported to interact with dysferlin.[26–32] These molecules are encoded by a fraction of genes such as *CAPN3*, *CAV3*, *DES*, *FLNC*, and *FHL1*, which are already known to cause myopathies. The remaining molecules may well be the next candidates. The identification of novel molecules that cause dysferlin deficiency can help elucidate the mechanisms by which dysferlin achieves membrane repair.

The study had a few limitations. The targeted genes in this study did not include the *DMD* gene, whose mutation is reported to result in secondary dysferlinopathy.[7] The immunoblot assay of muscle samples was not performed because muscle samples were not available. Thus, the quantitative level of dysferlin expression in sarcolemma or cytoplasm remains undetermined. The allelic zygosity of the multiple heterozygous candidate variants was not confirmed in all patients for the following reasons: (1) long-range PCR was unsuccessful if the distance between variants was too long or genomic DNA was estimated to be fragmented, or (2) there was a lack of available genomic parental DNA.

We used targeted next-generation sequencing to effectively and comprehensively analyze mutations in myopathy-associated genes and to clarify the heterogeneous nature of the genetic profile in patients with suspected dysferlinopathy. Our results illustrate the importance of comprehensive analysis of related genes when performing genetic diagnosis for dysferlinopathy. We believe that the genes and molecules responsible for the cases in which diagnosis remained unresolved will be identified by future whole-exome sequencing projects.

AUTHOR CONTRIBUTIONS

Rumiko Izumi: principal author, designed the study, analyzed and interpreted the data, drafted the manuscript. Tetsuya Niihori and Yoko Aoki: designed the study, analyzed and interpreted the data, and revised the manuscript. Toshiaki Takahashi: acquired and provided data, performed the Sanger sequencing, and revised the manuscript. Naoki Suzuki, Masaaki Kato, and Hitoshi Warita: revised the manuscript. Maki Tateyama: performed the immunohistochemical analysis of the biopsied muscles and revised the manuscript. Chigusa Watanabe, Kazuma Sugie, Hirotaka Nakanishi, and Gen Sobue: acquired and provided data. Masashi Aoki: designed the study, revised the manuscript, and acquired funding.

ACKNOWLEDGMENT

The authors thank the patients and their families and are grateful to Yoko Tateda, Kumi Kato, Naoko Shimakura, Risa Ando, Riyo Takahashi, and Chikako Yaginuma for their technical assistance. The authors also acknowledge the support of the Biomedical Research Core of Tohoku University Graduate School of Medicine.

STUDY FUNDING

This study was supported by an Intramural Research Grant (26-7 and 26-8) for Neurological and Psychiatric Disorders of NCNP; the grant on Research on Rare and Intractable Diseases (H26-intractable disease 037 and 082) from the Ministry of Health, Labour and Welfare of Japan; Grants-in-Aid for research on rare and intractable diseases from the Ministry of Health, Labour and Welfare of Japan (H26-nanchitou(nan)-ippan-079); Research Grant for Comprehensive Research on Disability Health and Welfare from the Ministry of Health, Labour and Welfare (H26-shinkei-kin-ippan-004); and Grant-in-Aid for Challenging Exploratory Research (26670436) from the Japanese Ministry of Education, Culture, Sports, Science and Technology.

DISCLOSURE

Dr. Izumi, Dr. Niihori, and Dr. Takahashi report no disclosures. Dr. Suzuki has received research support from Grant-in-Aid for Challenging Exploratory Research (26670436), Scientific Research B (25293199), and Young Scientists A (15H05667) from the Japanese Ministry of Education, Culture, Sports, Science and Technology. Dr. Tateyama has received honoraria for lecturing from Daiichi Sankyo company and has received research support from Japan Society for the Promotion of Science (JSPS). Dr. Watanabe, Dr. Sugie, and Dr. Nakanishi report no disclosures. Dr. Sobue has served on the scientific advisory boards of Kanae Science Foundation for the Promotion of Medical Science, the Naito Science Foundation, and the Takeda Foundation; has served on the editorial boards of *Brain, Degenerative Neurological and Neuromuscular Disease, Journal of Neurology*, and *Amyotrophic Lateral Sclerosis*; and has received research support from the Ministry of Education, Culture, Sports, Science and Technology of Japan; the Ministry of Welfare, Health and Labor of Japan; and the Japan Science and Technology Agency, Core Research for Evolutional Science and Technology. Dr. Kato reports no

disclosures. Dr. Warita has received research support from Grant-in-Aid for Scientific Research (26461288, 25293199, and 23591229) and Grant-in-Aid for Challenging Exploratory Research (26670436) from Japan Society for the Promotion of Science (JSPS), Japan. Dr. Y. Aoki has served on the editorial board for the *Journal of Human Genetics* and has received research support from the Japanese Foundation for Pediatric Research, the Japanese Ministry of Health Labor and Welfare, the Japan Society for the Promotion of Science (JSPS), and the Japan Agency for Medical Research and Development (AMED). Prof. M. Aoki has received research support from the Japanese Ministry of Health Labor and Welfare, NCNP, and the Japanese Ministry of Education, Culture, Sports, Science and Technology. Go to Neurology.org/ng for full disclosure forms.

Received August 24, 2015. Accepted in final form October 26, 2015.

REFERENCES

1. Aoki M, Liu J, Richard I, et al. Genomic organization of the dysferlin gene and novel mutations in Miyoshi myopathy. Neurology 2001;57:271–278.
2. Anderson LV, Davison K, Moss JA, et al. Dysferlin is a plasma membrane protein and is expressed early in human development. Hum Mol Genet 1999;8:855–861.
3. Bansal D, Miyake K, Vogel SS, et al. Defective membrane repair in dysferlin-deficient muscular dystrophy. Nature 2003;423:168–172.
4. Lennon NJ, Kho A, Bacskai BJ, Perlmutter SL, Hyman BT, Brown RH Jr. Dysferlin interacts with annexins A1 and A2 and mediates sarcolemmal wound-healing. J Biol Chem 2003;278:50466–50473.
5. Cacciottolo M, Numitone G, Aurino S, et al. Muscular dystrophy with marked Dysferlin deficiency is consistently caused by primary dysferlin gene mutations. Eur J Hum Genet 2011;19:974–980.
6. Matsuda C, Aoki M, Hayashi YK, Ho MF, Arahata K, Brown RH Jr. Dysferlin is a surface membrane-associated protein that is absent in Miyoshi myopathy. Neurology 1999;53:1119–1122.
7. Piccolo F, Moore SA, Ford GC, Campbell KP. Intracellular accumulation and reduced sarcolemmal expression of dysferlin in limb—girdle muscular dystrophies. Ann Neurol 2000;48:902–912.
8. Tagawa K, Ogawa M, Kawabe K, et al. Protein and gene analyses of dysferlinopathy in a large group of Japanese muscular dystrophy patients. J Neurol Sci 2003;211:23–28.
9. Matsuda C, Hayashi YK, Ogawa M, et al. The sarcolemmal proteins dysferlin and caveolin-3 interact in skeletal muscle. Hum Mol Genet 2001;10:1761–1766.
10. Tateyama M, Aoki M, Nishino I, et al. Mutation in the caveolin-3 gene causes a peculiar form of distal myopathy. Neurology 2002;58:323–325.
11. Chrobakova T, Hermanova M, Kroupova I, et al. Mutations in Czech LGMD2A patients revealed by analysis of calpain3 mRNA and their phenotypic outcome. Neuromuscul Disord 2004;14:659–665.
12. Hermanova M, Zapletalova E, Sedlackova J, et al. Analysis of histopathologic and molecular pathologic findings in Czech LGMD2A patients. Muscle Nerve 2006;33:424–432.
13. Groen EJ, Charlton R, Barresi R, et al. Analysis of the UK diagnostic strategy for limb girdle muscular dystrophy 2A. Brain 2007;130:3237–3249.
14. Takahashi T, Aoki M, Tateyama M, et al. Dysferlin mutations in Japanese Miyoshi myopathy: relationship to phenotype. Neurology 2003;60:1799–1804.
15. Takahashi T, Aoki M, Suzuki N, et al. Clinical features and a mutation with late onset of limb girdle muscular dystrophy 2B. J Neurol Neurosurg Psychiatry 2013;84:433–440.
16. Li H, Durbin R. Fast and accurate short read alignment with Burrows-Wheeler transform. Bioinformatics 2009;25:1754–1760.
17. McKenna A, Hanna M, Banks E, et al. The Genome Analysis Toolkit: a MapReduce framework for analyzing next-generation DNA sequencing data. Genome Res 2010;20:1297–1303.
18. Wang K, Li M, Hakonarson H. ANNOVAR: functional annotation of genetic variants from high-throughput sequencing data. Nucleic Acids Res 2010;38:e164.
19. Adzhubei IA, Schmidt S, Peshkin L, et al. A method and server for predicting damaging missense mutations. Nat Methods 2010;7:248–249.
20. Ng PC, Henikoff S. SIFT: predicting amino acid changes that affect protein function. Nucleic Acids Res 2003;31:3812–3814.
21. Cai H, Yabe I, Sato K, et al. Clinical, pathological, and genetic mutation analysis of sporadic inclusion body myositis in Japanese people. J Neurol 2012;259:1913–1922.
22. Kramerova I, Beckmann JS, Spencer MJ. Molecular and cellular basis of calpainopathy (limb girdle muscular dystrophy type 2A). Biochim Biophys Acta 2007;1772:128–144.
23. Anderson LV, Harrison RM, Pogue R, et al. Secondary reduction in calpain 3 expression in patients with limb girdle muscular dystrophy type 2B and Miyoshi myopathy (primary dysferlinopathies). Neuromuscul Disord 2000;10:553–559.
24. Angelini C, Nardetto L, Borsato C, et al. The clinical course of calpainopathy (LGMD2A) and dysferlinopathy (LGMD2B). Neurol Res 2010;32:41–46.
25. Ten Dam L, van der Kooi AJ, Rovekamp F, Linssen WH, de Visser M. Comparing clinical data and muscle imaging of DYSF and ANO5 related muscular dystrophies. Neuromuscul Disord 2014;24:1097–1102.
26. Huang Y, Verheesen P, Roussis A, et al. Protein studies in dysferlinopathy patients using llama-derived antibody fragments selected by phage display. Eur J Hum Genet 2005;13:721–730.
27. Matsuda C, Kameyama K, Tagawa K, et al. Dysferlin interacts with affixin (beta-parvin) at the sarcolemma. J Neuropathol Exp Neurol 2005;64:334–340.
28. Cacciottolo M, Belcastro V, Laval S, Bushby K, di Bernardo D, Nigro V. Reverse engineering gene network identifies new dysferlin-interacting proteins. J Biol Chem 2011;286:5404–5413.
29. Cai C, Weisleder N, Ko JK, et al. Membrane repair defects in muscular dystrophy are linked to altered interaction between MG53, caveolin-3, and dysferlin. J Biol Chem 2009;284:15894–15902.
30. Azakir BA, Di Fulvio S, Therrien C, Sinnreich M. Dysferlin interacts with tubulin and microtubules in mouse skeletal muscle. PLoS One 2010;5:e10122.
31. Flix B, de la Torre C, Castillo J, Casal C, Illa I, Gallardo E. Dysferlin interacts with calsequestrin-1, myomesin-2 and dynein in human skeletal muscle. Int J Biochem Cell Biol 2013;45:1927–1938.
32. de Morree A, Hensbergen PJ, van Haagen HH, et al. Proteomic analysis of the dysferlin protein complex unveils its importance for sarcolemmal maintenance and integrity. PLoS One 2010;5:e13854.

Neurology®
Genetics

Genetic profile for suspected dysferlinopathy identified by targeted next-generation sequencing

Rumiko Izumi, Tetsuya Niihori, Toshiaki Takahashi, et al.

Neurol Genet 2015;1;
DOI 10.1212/NXG.0000000000000036

Neuropathology and Applied Neurobiology (2015), **41**, 391–398 doi: 10.1111/nan.12179

Scientific correspondence

Clinicopathological features of the first Asian family having vocal cord and pharyngeal weakness with distal myopathy due to a *MATR3* mutation

Distal myopathy is a clinically and pathologically heterogeneous disorder that selectively or disproportionately affects distal muscles of the upper and/or lower limbs [1]. An adult-onset, progressive autosomal dominant distal myopathy that is frequently associated with dysphagia and dysphonia, vocal cord and pharyngeal weakness (VCPDM/MPD2) was recently discovered in a North American and a Bulgarian family; its causative agent being a missense mutation in the *matrin-3 (MATR3)* gene [2,3]. Still, VCPDM remains a fairly rare disease that has only been reported in two families worldwide so far.

According to a previous report on VCPDM, muscle biopsy performed on the quadriceps or gastrocnemius muscles revealed chronic non-inflammatory myopathy with subsarcolemmal rimmed vacuoles (RV) and atrophic fibres, with denervation [2]. Pathologic changes were reported to be more severe in the gastrocnemius than in the quadriceps muscles. Electrophysiological studies have also shown some degree of combination of myogenic and neurogenic changes associated with VCPDM [2].

Here, we report the clinicopathological features of the first Asian family having VCPDM with a missense mutation in the *MATR3* gene. We also examined whether muscle pathology in patients with VCPDM shared histopathological characteristics with other myopathies with RV, including sporadic inclusion body myositis (sIBM), oculopharyngeal muscular dystrophy (OPMD), glucosamine (UDP-N-acetyl)-2-epimerase/N-acetylmannosamine kinase (GNE) myopathy, and valosin-containing protein (VCP) myopathy.

Two Japanese half sisters were examined and summarized in Table 1. Their father noticed a disturbance in his gait in his forties and was dependent on a powered wheelchair in his sixties. He gradually developed respiratory problems and eventually underwent a tracheostomy with mechanical ventilation. He died of respiratory failure at 73.

Case 1, a 44-year-old woman experienced difficulty in ambulation and developed dysphagia of liquid and solids. Upon admission to our hospital, her neurological examination revealed dysphagia and dysarthria, while facial weakness and tongue atrophy were not observed. Moderate muscle weakness was detected in the neck flexor, and mild weakness without fasciculation was observed in the iliopsoas, hamstring, and tibialis anterior muscles. Touch and pinprick sensations were reduced in the distal upper and lower limbs, while vibration and position sense remained intact. Tendon reflexes, especially in the patella tendons, were generally weak.

Case 2, a 68-year-old woman (half sister of the patient in case 1) experienced difficulty in swallowing at age 63 and developed speech difficulty and finger weakness at age 65. Dysphagia and dysarthria progressed gradually until three months before hospital admission. After developing dyspnoea and somnolence, she was admitted to the hospital. Because of her respiratory dysfunction type 2 (PaO_2 50.5 mmHg, $PaCO_2$ 76.7 mmHg) diagnosis, she was treated with non-invasive positive pressure ventilation. Neurological examination showed dysphagia and nasal voice, despite there being no obvious facial weakness or tongue atrophy. Wasting was observed in the bilateral thenar, hypothenar, and first dorsal interossei muscles without fasciculation. The muscle weakness decreased moderately in the wrist extensors, iliopsoas, and extensor hallucis longus muscles and mildly in the deltoid, hamstring, and tibialis anterior muscles. Touch, pinprick, vibration, and position sensations remained intact but slight dysesthesia was present in the toe tips. Tendon reflexes were absent, except of a markedly decreased patella tendons reflex. Both cases of the patients did not fulfil diagnostic criteria of ALS because they lacked upper motor neurone signs.

After obtaining informed consent from patients and approval from a local ethics committee, genomic DNA was extracted from the peripheral blood samples for both patients. We conducted exome-sequencing to determine

Table 1. Summary of clinical data

	Case 1	*Case 2*
Age at biopsy	44	68
Age at onset	40	63
Gender	F	F
Distal weakness		
Legs	+	+
Hands	−	+
Shoulder weakness	−	+
Swallowing dysfunction	+	+
Vocal dysfunction	−	+
Respiratory dysfunction	−	+
CK (U/L, normal ranges: 45–176)	241	81
EMG	Myogenic + neurogenic	Myogenic + neurogenic
NCS	Axonal degeneration type sensorimotor polyneuropathy	Axonal degeneration type motorsensory polyneuropathy
Abnormal lesions in skeletal MRI	Gluteus, quadriceps, hamstring	Paraspinal, gluteus
%FVC (%)	58.9	36.0

the causative mutation for each patient. Exonic sequences were enriched using a SureSelect V4+UTR (Agilent) and subjected to massively parallel sequencing using Illumina Hiseq2000 (100 bp paired-end). Burrows Wheeler Aligner [4] and Samtools [5] were used for alignment and variation detection. It revealed a missense mutation in the *MATR3* gene: p.S85C (c.254C>G), which was exactly the same mutation as described in the only two previous families of VCPDM with a missense mutation in the *MATR3* gene by Senderek *et al.* [3]. Sanger sequencing confirmed this mutation for both cases.

In case 1, the patient underwent biopsy from the left biceps brachii muscle. Haematoxylin and eosin (HE) staining showed a severe fatty change in myofibres of various sizes (Figure 1**a**). Approximately 5% of myofibres presented myopathic changes with RV and internal nuclei (Figure 1**b**,**c**). Inflammatory cellular infiltrates were absent. Acid phosphatase staining showed weak activity consistent with lysosomal activity levels in the RV (Figure 1**d**). ATPase staining showed a predominance of type 1 fibres (Figure 1**e**,**f**). Neither upregulation of major histocompatibility complex (MHC) class I nor cytochrome c oxidase (COX)-negative muscle fibres was observed (data not shown).

In case 2, the patient underwent biopsy from the right biceps brachii muscle. HE staining showed that 1–2% of myofibres presented myopathic changes with RV and internal nuclei (Figure 1**g**,**h**). Inflammatory cellular infiltrates were not observed. Acid phosphatase staining showed no activity (Figure 1**i**). Interestingly, ATPase staining revealed a fibre-type grouping with an increase in type 2 fibres, indicating neurogenic changes (Figure 1**j–l**). The specimens showed no upregulation of MHC class I or COX-negative fibres (data not shown).

Electron microscopy of samples from case 1 demonstrated abundant autophagic vacuoles in degenerative myofibres (Figure 1**m**,**n**). As far as we could observe, we found no intranuclear aggregates (Figure 1**n**).

Next, we asked whether myopathic changes associated with VCPDM shared similar histopathological characteristics with myopathies with RV including sIBM, OPMD, GNE myopathy and VCP myopathy. The study was approved by the Ethics Committee of the Kumamoto University Hospital. Recent studies have shown that p62 is the best histological diagnostic marker for sIBM [6–9]. Therefore, we performed immunofluorescence staining using mouse anti-p62/SQSTM1 (1:250; Medical & Biological Laboratories, Nagoya, Japan) and rabbit anti-MATR3 (1:250; Bethyl Laboratories, Montgomery, TX, USA) antibodies. In healthy control subjects, p62 was not detected in normal muscle fibres (data not shown). Immunohistochemical analyses of p62 revealed its sarcoplasmic aggregates in 10–20% of the myofibres in patients with VCPDM (Figure 2**a**,**e**). Substantial immunoreactivity for p62 was observed in myofibres of patients with sIBM (Figure 2**i**), OPMD (Figure 2**m**) as well as GNE myopathy (Figure 2**q**) and VCP myopathy (Figure 2**u**). In healthy control subjects, all myonuclei stained for MATR3 (data not shown).

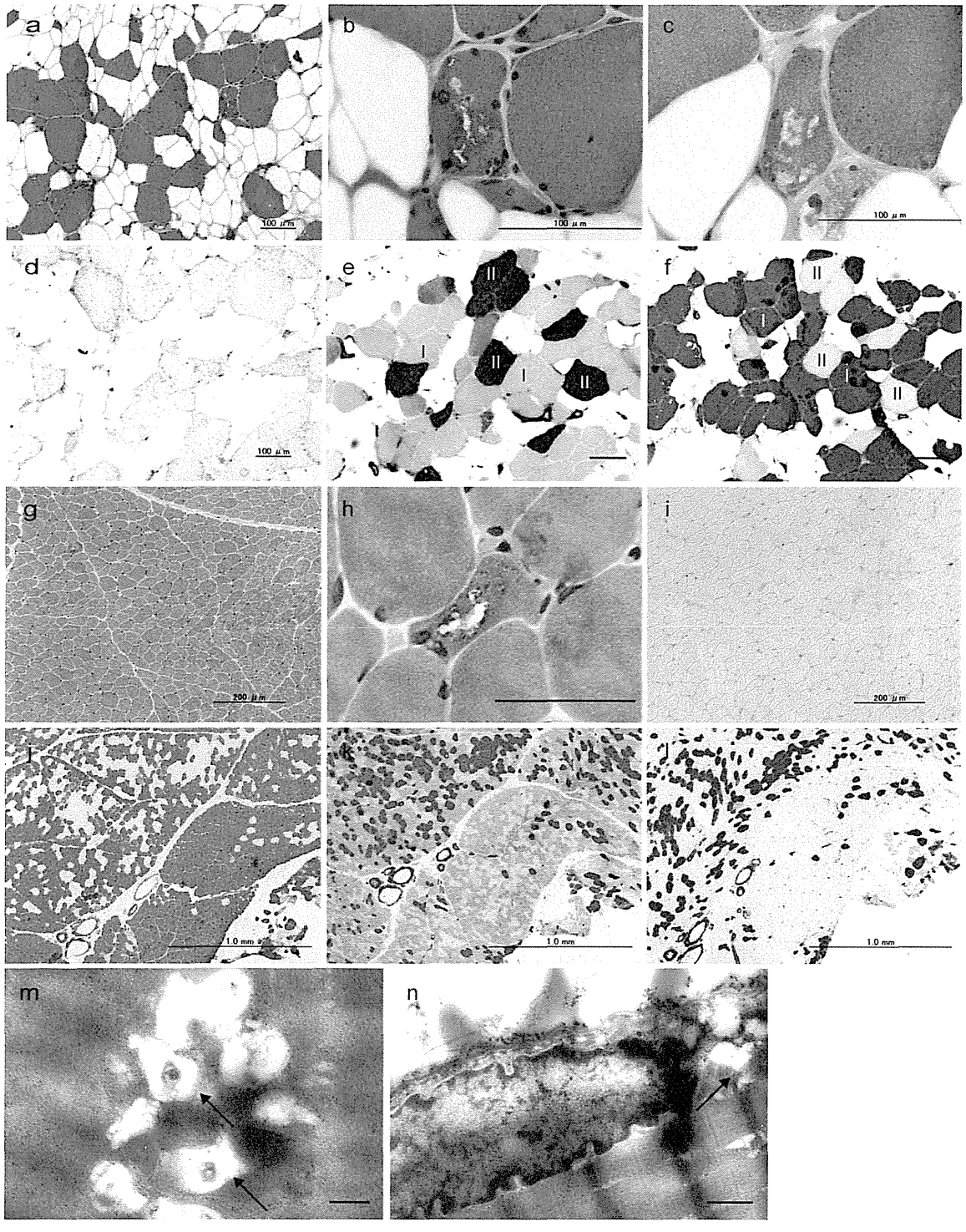

Figure 1. Muscle histology for the biopsy samples of VCPDM case 1 and 2. (**a–f**) VCPDM case 1: (**a**, **b**) Haematoxylin and eosin (HE) staining at lower (**a**) and higher (**b**) magnifications. (**c**) Modified Gomori-trichrome staining. (**d**) Acid phosphatase staining. (**e**, **f**) ATPase staining at pH 10.6 (**e**), and pH 4.2 (**f**). I and II indicate type 1 and 2 fibres, respectively. Scale bars = 100 μm. (**g–j**) VCPDM case 2: (**g**, **h**) HE staining at lower (**g**) and higher (**h**) magnifications. (**i**) Acid phosphatase staining. (**j–l**) ATPase staining at pH 10.7 (**j**), pH 4.5 (**k**) and pH 4.2 (**l**). Scale bars = 200 μm (**g**, **i**), 50 μm (**h**) and 1.0 mm (**j–l**). (**m**, **n**) Electron microscopic analysis of samples from VCPDM case 1. Arrows indicate autophagic vacuoles. Scale bars = 500 nm (**m**), 800 nm (**n**).

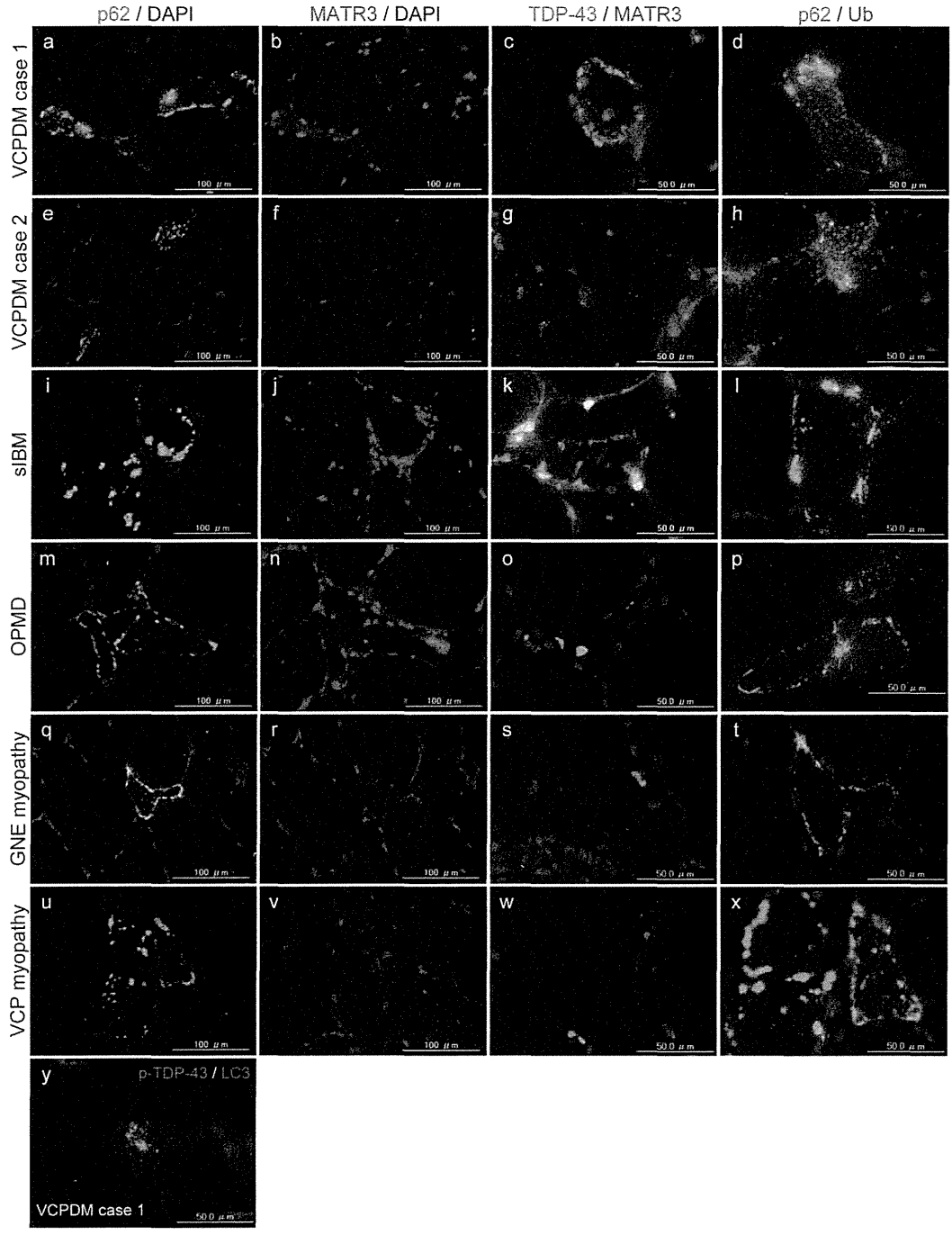

Figure 2. Immunofluorescence studies for proteins related to myopathies with rimmed vacuoles. Immunofluorescence study of p62 (green; **a**, **e**, **i**, **m**, **q**, **u**) and MATR3 (red; **b**, **f**, **j**, **n**, **r**, **v**) in identical specimens from VCPDM case 1 (**a**, **b**), case 2 (**e**, **f**), sIBM (**i**, **j**), OPMD (**m**, **n**), GNE myopathy with homozygous p.V572L mutation (**q**, **r**), and VCP myopathy with heterozygous p.A232E mutation (**u**, **v**). Double immunofluorescence study of TDP-43 (green) and MATR3 (red) in VCPDM case 1 (**c**), case 2 (**g**), sIBM (**k**), OPMD (**o**), GNE myopathy (**s**) and *VCP* myopathy (**w**). Double immunofluorescence study of p62 (green) and ubiquitin (red) in VCPDM case 1 (**d**), case 2 (**h**), sIBM (**l**), OPMD (**p**), GNE myopathy (**t**) and VCP myopathy (**x**). Double immunofluorescence study of phosphorylated TDP-43 (green) and LC-3 (red; 1: 500; Medical & Biological Laboratories, Nagoya, Japan) in VCPDM case 1(**y**). Immunolabelled proteins were visualized using anti-mouse immunoglobulin antibody-conjugated Alexa Fluor 488 or anti-rabbit immunoglobulin antibody-conjugated Alexa Fluor 594 (1:200; Life Technologies Corporation, Carlsbad, CA, USA). Scale bars = 100 μm (**a**, **b**, **e**, **f**, **m**, **n**, **q**, **r**, **u**, **v**) and 50 μm (**c**, **d**, **g**, **h**, **k**, **l**, **o**, **p**, **s**, **t**, **w**, **x**, **y**). Nuclei were stained with 4′, 6-diamidino-2-phenylindole (blue).

Table 2. Semi-quantitative analysis for immunohistochemistry

	p62	*MATR3*	*TDP-43*	*Ubiquitin*
VCPDM Case 1	++, aggregates	+, granular or loss of nuclear staining	++, aggregates	+, granular
VCPDM Case 2	++, aggregates	+, granular or loss of nuclear staining	±, diffuse	+, granular
sIBM	++, aggregates	±, granular	++, aggregates	+, granular
OPMD	++, aggregates	±, granular	++, aggregates	+, granular
GNE myopathy	++, aggregates	±, granular or loss of nuclear staining	+, aggregates	+, granular
VCP myopathy	++, aggregates	±, granular or loss of nuclear staining	++, aggregates	+, granular

VCPDM, vocal cord and pharyngeal weakness with distal myopathy; sIBM, sporadic inclusion body myositis; OPMD, oculopharyngeal muscular dystrophy. −, no positive cells; ±, occasional positive cells; +, moderate numbers of positive cells; ++, frequent numbers of positive cells.

Immunohistochemical analysis of MATR3 demonstrated sarcoplasmic granular staining in p62-positive degenerating myofibres for case 1 (Figure 2**b**). Some myonuclei showed a loss in immunoreactivity for MATR3 (Figure 2**b**). In case 2, some myonuclei presented immunoreactivity loss for MATR3 without sarcoplasmic staining (Figure 2**f**). Sarcoplasmic granular staining for MATR3 was observed in some p62-positive degenerating myofibres of patients with sIBM (Figure 2**j**), OPMD (Figure 2**n**), and GNE (Figure 2**r**) and VCP (Figure 2**v**) myopathies. Notably, most myonuclei remained strongly reactive to MATR3 in sIBM and OPMD, (Figure 2**j**,**n**) whereas some myonuclei showed a loss in immunoreactivity for MATR3 in GNE (Figure 2**r**) and VCP (Figure 2**v**) myopathies.

We then examined whether other proteins involved in RV-related myopathies accumulated in the myofibres of patients with VCPDM. Previous studies have shown frequent accumulation of TAR DNA-binding protein 43 kDa (TDP-43) in sarcoplasmic granules within degenerating myofibres of patients with sIBM (Figure 2**k**), OPMD (Figure 2**o**) and GNE (Figure 2**s**) and VCP (Figure 2**w**) myopathies. Within myofibres with TDP-43-immunoreactive sarcoplasmic aggregates, nuclei were less immunoreactive for TDP-43 in patients with sIBM (Figure 2**k**). An immunohistochemical analysis using mouse anti-TDP-43 (1: 250; ProteinTech Group, Chicago, IL, USA) antibody demonstrated the presence of its sarcoplasmic aggregates (~10%) in myofibres for Case 1 (Figure 2**c**) and diffuse cytoplasmic staining in myofibres for Case 2 (Figure 2**g**). In myofibres with TDP-43-positive aggregates in Case 1, myonuclei were less immunoreactive for both TDP-43 and MATR3, although both proteins did not necessarily colocalize (Figure 2**c**). Interestingly, some TDP-43-positive granules were immunoreactive for mouse anti-phosphorylated TDP-43 (pS409/410) (1: 3000; Cosmo Bio, Tokyo, Japan) antibody (Figure 2**y**).

Because a deficit in protein degradation machinery is suspected to be one of the pathophysiological mechanisms underlying RV-related myopathies, we investigated the involvement of ubiquitin in the myofibres of patients with VCPDM, using rabbit anti-ubiquitin (1: 200; Dako) antibody. In these patients, immunohistochemistry for ubiquitin showed sarcoplasmic granular staining mainly in p62-positive fibres (Figure 2**d**,**h**). Sarcoplasmic granular staining for ubiquitin was also observed in sIBM (Figure 2**l**), OPMD (Figure 2**p**) as well as GNE (Figure 2**t**) and VCP (Figure 2**x**) myopathies. Expression profiles are summarized in Table 2.

We herein reported clinicopathological features of the first Asian family having VCPDM with a missense mutation in the *MATR3* gene: p.S85C (c.254C>G), which was a sole mutation that has been described in the previous cases with VCPDM. Collectively, our results showed intrafamilial variation including the presentation of motorsensory neuropathy. We identified the histopathological characteristics of VCPDM: myopathic changes with RV but no inflammatory infiltrate, neurogenic changes, diffuse sarcoplasmic distribution of MATR3 and/or loss of nuclear staining, and other histological features common to RV-myopathies, such as accumulation of p62, TDP-43 and ubiquitin.

According to a previous report on the clinical features of VCPDM [2], muscle weakness is exhibited asymmetrically in the feet and ankles and/or the hands. The distribution of weakness in the lower limbs has been more affected in the peroneal muscles than in the gastrocnemius muscles. Weakness in the upper limbs occurs more often in the finger extensors and abductor pollicis brevis

(APB), and to lesser extent in the deltoid muscles. While vocal cord and pharyngeal weakness can be present at the onset of the distal weakness, some patients show neither vocal cord dysfunction nor problems swallowing. Our skeletal muscle MRI data indicated that the quadriceps muscles were relatively spared. Of note, the sparing of the vastus lateralis was described in another distal myopathy with RV, such as GNE myopathy [10], and the similarity might suggest the common pathogenesis between the both diseases.

Muscle histology in patients with VCPDM has previously revealed chronic non-inflammatory myopathy in addition to the presence of RV, usually in subsarcolemmal as well as atrophic fibres [2]. However, the specific characteristics of VCPDM have still not been conclusively determined. TDP-43 has been identified as a major component protein of ubiquitin-positive inclusions in the brains of patients with frontotemporal lobar degeneration with ubiquitin-positive inclusions and in the spinal anterior horns of patients with amyotrophic lateral sclerosis (ALS) [11,12]. TDP-43-positive granules have been observed not only in sIBM but also in other vacuolar myopathies such as OPMD, and VCP and GNE myopathies [7,13–17]. Our observation of TDP-43-positive granules in VCPDM suggests that the presence of TDP-43-positive aggregates may be a common phenomenon among myopathies associated with RV [8,13,14,17,18].

MATR3 is a component of the nuclear matrix and thought to be associated with the protein machinery for transcription, RNA splicing and DNA replication [3]. To date, the mutation of p.S85C (c.254C>G) in the *MATR3* gene is a sole mutation described in the previous cases with VCPDM. Recent exome-sequencing study has revealed mutations in the *MATR3* gene in some of ALS kindreds [19]. Interestingly, the report included one of the families harbouring the S85C mutation that had been originally described as having myopathy due to the *MATR3* mutation [3], and reclassified the condition as slowly progressive familial ALS. However, we provide definite evidence that the S85C *MATR3* mutation actually induced distal myopathy with minor neurogenic features. Taken together with these observations, the *MATR3* mutation can indeed cause wide-ranged phenotypes from inclusion body myopathy to motor neurone disease.

Although MATR3 is a multifunctional protein [19], the effect of the mutation on structure and function of MATR3 protein remains unsolved. Our observation of the sarcoplasmic accumulation of p62, TDP-43, and ubiquitin suggests a deficit in protein degradation, possibly due to ubiquitin proteasome system dysfunction and/or autophagy. Furthermore, the findings that immunoreactivity loss for MATR3 in the myonuclei was related with its sarcoplasmic staining might suggest that the mutation in the *MATR3* gene interferes directly or indirectly with the protein localization resulting in loss-of-function. The dysfunction of MATR3 by its mutation would possibly lead to a modification in gene expression related to abnormal chromatin organization, deregulation of nuclear mRNA export, abnormal pre-mRNA splicing, or nuclear proteome alterations in skeletal muscles. As *MATR3* knockdown caused deficit in the machinery for DNA damage response and cell cycle [20], such a nuclear dysfunction might be involved in VCPDM pathogenesis. Further investigation and establishing an understanding of the *MATR3* mutation in transgenic animals will be necessary to elucidate the pathophysiological mechanisms underlying myofibre degeneration and neuropathic change.

Acknowledgements

We would like to thank Ms Oka and all members of Department of Neurology, Kumamoto University Hospital for the technical help with muscle biopsies and clinical data collection. This research was supported by a Grant-in-Aid for Scientific Research (C), the Ministry of Education, Culture, Sports, Science and Technology of Japan; Grants-in-Aid from the Research on Intractable Diseases, Ministry of Health, Labor and Welfare of Japan; and Grants-in-Aid from the Research Committee for Applying Health and Technology of Ministry of Health, Welfare and Labor, Japan.

Authors' contribution

SY and AM: conception, design, acquisition of data, analysis and interpretation. YN, RK, NT, TN, YM, HU, SI, YH, AH, IH, SM and JY: acquisition of data. MU, HT and ST: acquisition of data and critical revision of the manuscript for important intellectual content. AY: analysis and interpretation, critical revision of the manuscript for important intellectual content and study supervision.

Conflict of interest

The authors declare that they have no conflict of interest.

S. Yamashita*
A. Mori*
Y. Nishida†
R. Kurisaki‡
N. Tawara*
T. Nishikami*
Y. Misumi*
H. Ueyama†
S. Imamura†
Y. Higuchi§
A. Hashiguchi§
I. Higuchi§
S. Morishita¶
J. Yoshimura¶
M. Uchino*
H. Takashima§
S. Tsuji**
Y. Ando*

**Department of Neurology, Graduate School of Medical Sciences, Kumamoto University, †Department of Neurology, National Hospital Organization, Kumamoto Saishunsou National Hospital, ‡Department of Neurology, National Hospital Organization, Kumamoto Minami National Hospital, Kumamoto, §Department of Neurology and Geriatrics, Kagoshima University Graduate School of Medical and Dental Sciences, Kagoshima, and ¶Department of Computational Biology, Graduate School of Frontier Sciences and **Department of Neurology, Graduate School of Medicine, The University of Tokyo, Tokyo, Japan*

References

1 Udd B. Distal myopathies–new genetic entities expand diagnostic challenge. *Neuromuscul Disord* 2012; **22**: 5–12
2 Feit H, Silbergleit A, Schneider LB, Gutierrez JA, Fitoussi RP, Reyes C, Rouleau GA, Brais B, Jackson CE, Beckmann JS, Seboun E. Vocal cord and pharyngeal weakness with autosomal dominant distal myopathy: clinical description and gene localization to 5q31. *Am J Hum Genet* 1998; **63**: 1732–42
3 Senderek J, Garvey SM, Krieger M, Guergueltcheva V, Urtizberea A, Roos A, Elbracht M, Stendel C, Tournev I, Mihailova V, Feit H, Tramonte J, Hedera P, Crooks K, Bergmann C, Rudnik-Schoneborn S, Zerres K, Lochmuller H, Seboun E, Weis J, Beckmann JS, Hauser MA, Jackson CE. Autosomal-dominant distal myopathy associated with a recurrent missense mutation in the gene encoding the nuclear matrix protein, matrin 3. *Am J Hum Genet* 2009; **84**: 511–18
4 Li H, Durbin R. Fast and accurate short read alignment with Burrows-Wheeler transform. *Bioinformatics* 2009; **25**: 1754–60
5 Li H, Handsaker B, Wysoker A, Fennell T, Ruan J, Homer N, Marth G, Abecasis G, Durbin R. The Sequence Alignment/Map format and SAMtools. *Bioinformatics* 2009; **25**: 2078–9
6 Dubourg O, Wanschitz J, Maisonobe T, Behin A, Allenbach Y, Herson S, Benveniste O. Diagnostic value of markers of muscle degeneration in sporadic inclusion body myositis. *Acta Myol* 2011; **30**: 103–8
7 Weihl CC, Pestronk A. Sporadic inclusion body myositis: possible pathogenesis inferred from biomarkers. *Curr Opin Neurol* 2010; **23**: 482–8
8 D'Agostino C, Nogalska A, Engel WK, Askanas V. In sporadic inclusion body myositis muscle fibres TDP-43-positive inclusions are less frequent and robust than p62 inclusions, and are not associated with paired helical filaments. *Neuropathol Appl Neurobiol* 2011; **37**: 315–20
9 Nogalska A, Terracciano C, D'Agostino C, King Engel W, Askanas V. p62/SQSTM1 is overexpressed and prominently accumulated in inclusions of sporadic inclusion-body myositis muscle fibers, and can help differentiating it from polymyositis and dermatomyositis. *Acta Neuropathol* 2009; **118**: 407–13
10 Tasca G, Ricci E, Monforte M, Laschena F, Ottaviani P, Rodolico C, Barca E, Silvestri G, Iannaccone E, Mirabella M, Broccolini A. Muscle imaging findings in GNE myopathy. *J Neurol* 2012; **259**: 1358–65
11 Neumann M, Sampathu DM, Kwong LK, Truax AC, Micsenyi MC, Chou TT, Bruce J, Schuck T, Grossman M, Clark CM, McCluskey LF, Miller BL, Masliah E, Mackenzie IR, Feldman H, Feiden W, Kretzschmar HA, Trojanowski JQ, Lee VM. Ubiquitinated TDP-43 in frontotemporal lobar degeneration and amyotrophic lateral sclerosis. *Science* 2006; **314**: 130–3
12 Arai T, Hasegawa M, Akiyama H, Ikeda K, Nonaka T, Mori H, Mann D, Tsuchiya K, Yoshida M, Hashizume Y, Oda T. TDP-43 is a component of ubiquitin-positive tau-negative inclusions in frontotemporal lobar degeneration and amyotrophic lateral sclerosis. *Biochem Biophys Res Commun* 2006; **351**: 602–11
13 Weihl CC, Temiz P, Miller SE, Watts G, Smith C, Forman M, Hanson PI, Kimonis V, Pestronk A. TDP-43 accumulation in inclusion body myopathy muscle suggests a common pathogenic mechanism with frontotemporal dementia. *J Neurol Neurosurg Psychiatry* 2008; **79**: 1186–9
14 Salajegheh M, Pinkus JL, Taylor JP, Amato AA, Nazareno R, Baloh RH, Greenberg SA. Sarcoplasmic redistribution of nuclear TDP-43 in inclusion body myositis. *Muscle Nerve* 2009; **40**: 19–31
15 Olive M, Janue A, Moreno D, Gamez J, Torrejon-Escribano B, Ferrer I. TAR DNA-Binding protein 43 accumulation in protein aggregate myopathies. *J Neuropathol Exp Neurol* 2009; **68**: 262–73

16 Kusters B, van Hoeve BJ, Schelhaas HJ, Ter Laak H, van Engelen BG, Lammens M. TDP-43 accumulation is common in myopathies with rimmed vacuoles. *Acta Neuropathol* 2009; **117**: 209–11
17 Yamashita S, Kimura E, Tawara N, Sakaguchi H, Nakama T, Maeda Y, Hirano T, Uchino M, Ando Y. Optineurin is potentially associated with TDP-43 and involved in the pathogenesis of inclusion body myositis. *Neuropathol Appl Neurobiol* 2013; **39**: 406–16
18 Neumann M, Mackenzie IR, Cairns NJ, Boyer PJ, Markesbery WR, Smith CD, Taylor JP, Kretzschmar HA, Kimonis VE, Forman MS. TDP-43 in the ubiquitin pathology of frontotemporal dementia with VCP gene mutations. *J Neuropathol Exp Neurol* 2007; **66**: 152–7
19 Johnson JO, Pioro EP, Boehringer A, Chia R, Feit H, Renton AE, Pliner HA, Abramzon Y, Marangi G, Winborn BJ, Gibbs JR, Nalls MA, Morgan S, Shoai M, Hardy J, Pittman A, Orrell RW, Malaspina A, Sidle KC, Fratta P, Harms MB, Baloh RH, Pestronk A, Weihl CC, Rogaeva E, Zinman L, Drory VE, Borghero G, Mora G, Calvo A, Rothstein JD, Drepper C, Sendtner M, Singleton AB, Taylor JP, Cookson MR, Restagno G, Sabatelli M, Bowser R, Chio A, Traynor BJ. Mutations in the Matrin 3 gene cause familial amyotrophic lateral sclerosis. *Nat Neurosci* 2014; **17**: 664–6
20 Salton M, Lerenthal Y, Wang SY, Chen DJ, Shiloh Y. Involvement of Matrin 3 and SFPQ/NONO in the DNA damage response. *Cell Cycle* 2010; **9**: 1568–76

Received 17 April 2014
Accepted after revision 13 August 2014
Published online Article Accepted on 4 September 2014

Available online at www.sciencedirect.com

ScienceDirect

Neuromuscular Disorders 25 (2015) 60–69

www.elsevier.com/locate/nmd

Congenital myasthenic syndrome in Japan: Ethnically unique mutations in muscle nicotinic acetylcholine receptor subunits

Yoshiteru Azuma [a,b], Tomohiko Nakata [a,b], Motoki Tanaka [c], Xin-Ming Shen [d], Mikako Ito [a], Satoshi Iwata [a], Tatsuya Okuno [a], Yoshiko Nomura [e], Naoki Ando [f], Keiko Ishigaki [g], Bisei Ohkawara [a], Akio Masuda [a], Jun Natsume [b], Seiji Kojima [b], Masahiro Sokabe [c], Kinji Ohno [a,*]

[a] *Division of Neurogenetics, Center for Neurological Diseases and Cancer, Nagoya University Graduate School of Medicine, Nagoya, Japan*
[b] *Department of Pediatrics, Nagoya University Graduate School of Medicine, Nagoya, Japan*
[c] *Department of Physiology, Nagoya University Graduate School of Medicine, Nagoya, Japan*
[d] *Department of Neurology, Mayo Clinic, Rochester, MN, USA*
[e] *Segawa Neurological Clinic for Children, Tokyo, Japan*
[f] *Department of Pediatrics, Nagoya City University Graduate School of Medicine, Nagoya, Japan*
[g] *Department of Pediatrics, Tokyo Women's Medical University, Tokyo, Japan*

Received 29 May 2014; received in revised form 9 August 2014; accepted 3 September 2014

Abstract

Congenital myasthenic syndromes (CMS) are caused by mutations in genes expressed at the neuromuscular junction. Most CMS patients have been reported in Western and Middle Eastern countries, and only four patients with *COLQ* mutations have been reported in Japan. We here report six mutations in acetylcholine receptor (AChR) subunit genes in five Japanese patients. Five mutations are novel, and one mutation is shared with a European American patient but with a different haplotype. Among the observed mutations, p.Thr284Pro (p.Thr264Pro according to the legacy annotation) in the epsilon subunit causes a slow-channel CMS. Five other mutations in the delta and epsilon subunits are splice site, frameshift, null, or missense mutations causing endplate AChR deficiency. We also found a heteroallelic p.Met465Thr in the beta subunit in another patient. p.Met465Thr, however, was likely to be polymorphism, because single channel recordings showed mild shortening of channel openings without affecting cell surface expression of AChR, and the minor allelic frequency of p.Met465Thr was 5.1% in the Japanese population. Lack of shared mutant alleles between the Japanese and the other patients suggests that most mutations described here are ethnically unique or *de novo* in each family.

Keywords: Congenital myasthenic syndromes; Acetylcholine receptor; Slow channel syndrome; Fast channel syndrome; Endplate acetylcholine receptor deficiency

1. Introduction

Acetylcholine released from the nerve terminal binds to muscle nicotinic acetylcholine receptor (AChR) at the motor endplate. AChR is clustered at the neuromuscular junction (NMJ) by binding to rapsyn with a stoichiometry of rapsyn to AChR of 1:1 to 2:1 [1]. AChR clustering is mediated by neural agrin that is released from the nerve terminal [2]. In early embryonic development, AChR clustering is also mediated by Wnt ligands [3,4]. Embryonic AChR is composed of α, β, δ, and γ subunits with a stoichiometry of $\alpha_2\beta\delta\gamma$. After birth, the ε subunit is substituted for the γ subunit, generating $\alpha_2\beta\delta\varepsilon$-AChR.

Congenital myasthenic syndromes (CMS) are heterogeneous disorders caused by mutations in genes expressed at the NMJ [5]. They are characterized by fatigable muscle weakness, variable muscle atrophy, and sometimes dysmorphic features. CMS mutations have been reported in 19 genes, with most mutations in *CHRNA1*, *CHRNB1*, *CHNRD*, and *CHNRE* encoding the AChR α, β, δ, and ε subunits, respectively. These mutations fall into three subsets: i) slow-channel CMS (SCCMS), in which the open time of AChR is abnormally prolonged; ii) fast-channel CMS (FCCMS), in which the open time of AChR is abnormally brief; and iii) endplate AChR deficiency. SCCMS is caused by a gain-of-function mutation and is dominantly inherited with variable penetrance [6]. In contrast, FCCMS and endplate AChR deficiency are caused by loss-of-function mutations on both alleles, and are recessively

* Corresponding author. Division of Neurogenetics, Center for Neurological Disease and Cancer, Nagoya University Graduate School of Medicine, 65 Tsurumai, Showa-ku, Nagoya 466-8550, Japan. Tel.: +81 52 744 2446; fax: +81 52 744 2449.
E-mail address: ohnok@med.nagoya-u.ac.jp (K. Ohno).

http://dx.doi.org/10.1016/j.nmd.2014.09.002
0960-8966/